Molecular BioSystems

Dynamic Article Links

Cite this: *Mol. BioSyst.*, 2011, **7**, 3065–3074

www.rsc.org/molecularbiosystems

PAPER

Proteomic analysis of gemcitabine-induced drug resistance in pancreatic cancer cells†

Yi-Wen Chen,[a] Jieh-Yuan Liu,[b] Szu-Ting Lin,[a] Ji-Min Li,[a] Shun-Hong Huang,[a] Jing-Yi Chen,[c] Jing-Yiing Wu,[ad] Cheng-Chin Kuo,[d] Chieh-Lin Wu,[a] Ying-Chieh Lu,[a] You-Hsuan Chen,[a] Chiao-Yuan Fan,[a] Ping-Chun Huang,[a] Ching-Hsuan Law,[a] Ping-Chiang Lyu,*[a] Hsiu-Chuan Chou*[c] and Hong-Lin Chan*[a]

Received 30th March 2011, Accepted 16th August 2011
DOI: 10.1039/c1mb05125c

Currently, the most effective agent against pancreatic cancer is gemcitabine (GEM), which inhibits tumor growth by interfering with DNA replication and blocking DNA synthesis. However, GEM-induced drug resistance in pancreatic cancer compromises the therapeutic efficacy of GEM. To investigate the molecular mechanisms associated with GEM-induced resistance, 2D-DIGE and MALDI-TOF mass spectrometry were performed to compare the proteomic alterations of a panel of differential GEM-resistant PANC-1 cells with GEM-sensitive pancreatic cells. The proteomic results demonstrated that 33 proteins were differentially expressed between GEM-sensitive and GEM-resistant pancreatic cells. Of these, 22 proteins were shown to be resistance-specific and dose-dependent in the regulation of GEM. Proteomic analysis also revealed that proteins involved in biosynthesis and detoxification are significantly over-expressed in GEM-resistant PANC-1 cells. In contrast, proteins involved in vascular transport, bimolecular decomposition, and calcium-dependent signal regulation are significantly over-expressed in GEM-sensitive PANC-1 cells. Notably, both protein–protein interaction of the identified proteins with bioinformatic analysis and immunoblotting results showed that the GEM-induced pancreatic cell resistance might interplay with tumor suppressor protein p53. Our approach has been shown here to be useful for confidently detecting pancreatic proteins with differential resistance to GEM. Such proteins may be functionally involved in the mechanism of chemotherapy-induced resistance.

Introduction

Drug resistance reduces the effectiveness of drugs in curing diseases such as cancer. In clinical practice, drug resistance becomes a serious problem when the dosages of anticancer compounds that are required to kill tumor cells increase to an uncontrollable concentration. The biological processes of drug resistance have been described before, including the enhanced activity of membrane-embedded drug extrusion pumps such as adenosine triphosphate-binding cassette (ABC)-transporters, the alteration of drug targeting DNA repair pathways, and the modulation of cell death signal transduction pathways.[1] The prognosis of pancreatic cancer is still poor as a consequence of the cancer's aggressiveness and the lack of effective therapies in the early stages.[2] Therefore, this disease is usually diagnosed at the time of progression, with a 1 to 4% five-year survival rate after diagnosis. Pancreatic cancer is resistant to almost all classes of chemotherapeutic drugs.[3] Currently, the most effective agent against pancreatic cancer is gemcitabine (GEM), which inhibits tumor growth by replacing cytidine during DNA replication and blocking the biosynthesis of deoxyribonucleotide by inactivating ribonucleotide reductase.[4] However, GEM-induced drug resistance of pancreatic cancer cells impacts on the therapeutic effect of GEM.[5] Thus, a better understanding of the molecular mechanisms of GEM resistance is essential to allow GEM to be used more effectively. Proteomics is a powerful tool for investigating proteins whose expressions are different between drug-sensitive and drug-resistant cells. 2-DE is currently a crucial technique in proteomics to profile thousands of proteins

[a] *Institute of Bioinformatics and Structural Biology & Department of Medical Sciences, National Tsing Hua University, Hsinchu, Taiwan. E-mail: pclyu@mx.nthu.edu.tw, hlchan@life.nthu.edu.tw; Fax: +886-3-5715934; Tel: +886-3-5742762, +886-3-5742476*
[b] *National Institute of Cancer Research, National Health Research Institutes, Zhunan Town, Miaoli 350, Taiwan*
[c] *Department of Applied Science, National Hsinchu University of Education, Hsinchu, Taiwan. E-mail: chouhc@mail.nhcue.edu.tw; Fax: +886-3-5257178, +886-3-5715934; Tel: +886-3-5213132ext2721*
[d] *Institute of Cellular and System Medicine, National Health Research Institutes, Zhunan, Miaoli, Taiwan*
† Electronic supplementary information available (ESI). See DOI: 10.1039/c1mb05125c

within biological samples and plays a complementary role in LC/MS-based proteomic analysis.[6] However, reliable quantitative comparisons between gels and gel-to-gel variations remain the primary challenge in 2-DE analysis. A significant improvement in the gel-based analysis of protein quantitation and detection was achieved by the introduction of 2D-DIGE, which can co-detect numerous samples in the same 2-DE. This approach minimizes gel-to-gel variations and compares the relative amount of protein features across different gels using an internal fluorescent standard. Moreover, the 2D-DIGE technique has the advantages of a broader dynamic range, higher sensitivity, and greater reproducibility than traditional 2-DE.[6] This innovative technology relies on the pre-labeling of protein samples with fluorescent dyes (Cy2, Cy3 and Cy5) before electrophoresis. Each dye has a distinct fluorescent wavelength, allowing multiple experimental samples with an internal standard to be simultaneously separated in the same gel. The internal standard, which is a pool of an equal amount of the experimental protein samples, helps provide accurate normalization data and increase statistical confidence in relative quantification across gels.[7–11] To thoroughly understand the molecular mechanisms associated with GEM-induced resistance, a global proteomic analysis of GEM-sensitive and GEM-resistant pancreatic cells is important. Accordingly, we established a panel of differential GEM-resistant PANC-1 cells by stepwise increase in the concentration of GEM in culture medium. The resistant PANC-1 cells can grow in 300 nM and 1500 nM of GEM. This study used 2D-DIGE and MALDI-TOF mass spectrometry to investigate the pancreatic proteins related to GEM-resistance.

Results

In this study, GEM-resistant PANC-1 cell lines were established with stepwise increase in the GEM concentration in a culture medium. These resistant PANC-1 cells can regularly grow in either 300 nM (GEM 300) or 1500 nM (GEM 1500) of GEM with no reduction in cell viability (data not shown). To study the alterations of cellular proteins in differential GEM-resistant lines, comparative proteomic analysis was performed across GEM 300/GEM 1500-resistant lines and GEM-sensitive PANC-1 cells. Protein samples were minimally labeled with Cy3 and Cy5 dyes and distributed to each gel. A pool of both samples was also prepared for labeling, with Cy2 as an internal standard to run on all gels to facilitate image matching across gels.

Thus, the triplicate samples resolved in different gels could be quantitatively analyzed using the internal standard on multiple 2-DE. After resolving protein samples with the 2D-DIGE technique, the DeCyder image analysis software indicated that 2815 protein features were detected while 221 protein features across any two conditions showed greater than a 1.3-fold change in the expression level with the student *t*-test (p-value < 0.05). MALDI-TOF MS identification revealed that 33 proteins were differentially expressed (circled spots in Fig. 1 and Table 1).

To visually display alterations in corresponding spot intensity proportions, representative identified spots (annexin A4 and acyl-coenzyme A synthetase) were shown as 2D protein maps and 3D images. The expression changes of standardized abundance in selected protein spots by DeCyder software were also shown (Fig. 2). In addition, peptide mass fingerprints of representative identified proteins, annexin A4 and acyl-coenzyme A synthetase, were shown in Fig. 3.

2D-DIGE, ELISA and immunoblotting analysis were then performed to confirm the differential expression levels of cathepsin D, ribonuclease inhibitor, heat shock protein β-1 (HSP27), and ribonucleoside-diphosphate reductase (RDR) (Fig. 4). Expression levels of cathepsin D were steadily down-regulated in response to the increase in GEM-resistance (Fig. 4A). In contrast, expression levels of RDR showed significant upregulation in correlation with an increase in GEM-resistance (Fig. 4C). These results are consistent with our previous proteomic data. Additionally, ribonuclease inhibitor and HSP27 were both downregulated at GEM 300. However, only HSP27 was restored to the basal level at GEM 1500, while the expression of ribonuclease inhibitor did not completely restore at GEM 1500 (Fig. 4B and C). Notably, a significant molecular weight shift of HSP27 was observed at GEM 1500, suggesting that post-translational modifications might occur on HSP27 (Fig. 4C).

According to the STRING protein interaction database (http://string.embl.de/), and using the identified proteins as inputs, a substantial portion of the proteins identified have been reported to be confidently associated with the tumor suppressor protein p53, including cathepsin D,[13] deoxyuridine 5'-triphosphate nucleotidohydrolase,[14] DNA-repair protein XRCC2,[15] HSP27,[16] heat shock protein HSP 90-β,[17] heterogeneous nuclear ribonucleoproteins A2/B1,[18] NAD(P)H dehydrogenase 1,[19] and ribonucleoside-diphosphate reductase[20] (Fig. 5A).

The interaction map in Fig. 5A shows at the 'medium' confidence level that a significant number (10/33; 30.3%) of the entered proteins can interact with the p53 protein. This interpretation has further been supported by immunoblotting analysis, demonstrating that levels of p53 proteins correlated negatively with the development of GEM-resistant pancreatic cells (Fig. 5B).

Discussion

The results of this study showed the differentially expressed protein profiles across GEM-sensitive and GEM 300/GEM 1500-resistant cells. We used the 2D-DIGE strategy for large-scale protein quantification in this study, which was sufficiently powerful to identify numerous GEM-resistant signatures. In addition, 2D-DIGE offers a complementary role to LC MS-based proteomic analysis.

Though the global coverage of protein mixtures identified by LC/MS-based analysis is generally higher than that of 2-DE-based analysis, 2-DE-based analysis offers a number of distinct advantages, such as direct protein quantification at protein isoform levels instead of peptide levels to reduce analytical variations.[6] Proteomic analysis using large-scale 2D-DIGE with 24 cm IPG strips demonstrated that 221 protein features were differentially expressed across GEM-resistant PANC-1 lines and the GEM-sensitive PANC-1 line. Of these, 33 features were identified by MALDI-TOF MS, corresponding to 29 unique proteins.

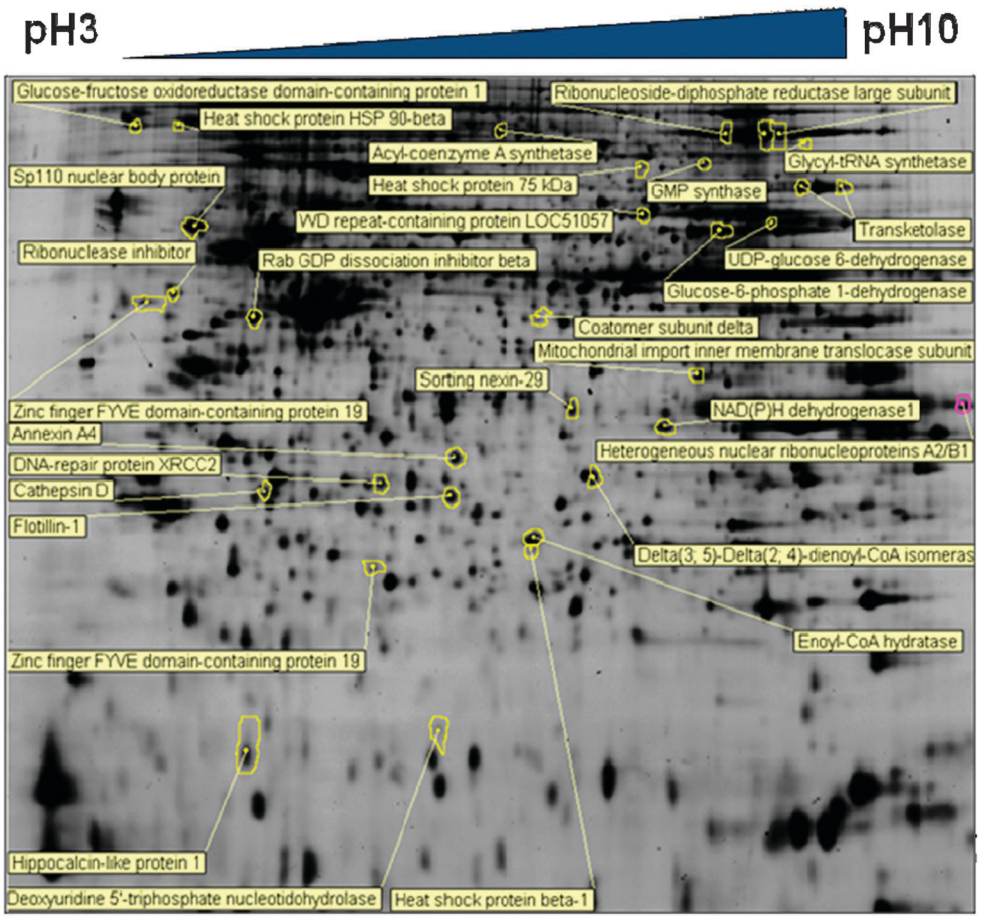

Fig. 1 2D-DIGE analysis of differentially expressed protein profiling in response to various levels of gemcitabine-induced drug resistance. Protein samples (100 μg each) were labeled with Cy-dyes and separated using 24 cm, pH 3–10 non-linear IPG strips. 2D-DIGE images of the cell samples from various levels of gemcitabine-induced drug resistance were analyzed with DeCyder software, and the differentially expressed identified protein features are annotated with circles.

Notably, 22 out of the 33 identified GEM-resistance specific proteins showed resistance-dependent upregulation or downregulation behavior (Table 1). For example, protein spot 376, identified as a ribonucleoside-diphosphate reductase large subunit, was 23.48-fold upregulated in GEM (300) and 43.30-fold upregulated in GEM (1500). In addition, protein spot 1254, identified as rab GDP dissociation inhibitor β, was 1.54-fold downregulated in GEM (300) and 3.30-fold downregulated in GEM (1500) (Table 1). These data confirm that these identified proteins are closely related to, if not completely responsible for, GEM-resistance.

In addition to being incorporated into DNA to interfere with DNA synthesis, GEM enhances its cytotoxicity by inhibiting ribonucleotide-diphosphate reductase, which is an enzyme that catalyzes the formation of deoxyribonucleotides from ribonucleotides. Consequently, the enhanced activity or overexpression of ribonucleotide-diphosphate reductase is expected in GEM-induced drug resistance. In the current study, we observed that the protein expression of ribonucleotide-diphosphate reductase increased more than 40-fold in GEM1500 and 20-fold in GEM300. In addition, recent publications have indicated that the increased expression of ribonucleotide reductase is involved in gemcitabine resistance in numerous cell systems.[21–23] Thus, our proteomic results display good correlation with these reports. Furthermore, our established gemcitabine resistance model is reliable for the analysis of gemcitabine-induced drug resistance. Based on a Swiss-Prot search and KEGG pathway analysis, numerous potential biological functions of the identified proteins across GEM-resistant PANC-1 lines and the GEM-sensitive PANC-1 line were determined. This information should be useful for studying the mechanisms of GEM-induced drug resistance. Table 2 compares the expression profiles of the identified differentially expressed proteins in these cell lines. Proteins known to regulate fatty acid biosynthesis and fatty acid biodegradation are found to be upregulated and downregulated, respectively, in resistant PANC-1. In addition, the expression of proteins linked to protein synthesis and protein degradation increased and decreased, respectively, in resistant PANC-1 cells in comparison to the levels in sensitive PANC-1 cells. Proteomic analysis also revealed that proteins involved in DNA synthesis and detoxification are significantly overexpressed in resistant PANC-1 cells. In contrast, proteins involved in vascular transport and calcium-dependent signal regulation are significantly downregulated in resistant PANC-1 cells (Table 2). In brief, metabolic pathways responsible for biomolecule synthesis are upregulated while pathways responsible for biomolecule degradation are downregulated.

Table 1 Alphabetical list of identified differentially expressed proteins across various levels of gemcitabine-induced drug resistant PANC-1 pancreatic cells obtained after 2D-DIGE coupled with MALDI-TOF mass spectrometry analysis

No.	Accession no.	Protein name	pI	MW	No. match. peptides	Cov. (%)	Score	GEM300/ Ctrol	*t*-Test	GEM1500/ Ctrl	*t*-Test	Matched peptides	Functional classification
316	Q68CK6	Acyl-coenzyme A synthetase ACSM2B, mitochondrial	8.5	64 786	5/13	10	56/56	1.37	0.005	1.9	0.0056	GIKDEDGYFQFMGR-SCDGWLNFK	Fatty acid biosynthetase
1744	P09525	Annexin A4	5.84	36 088	8/14	20	85/56	−1.55	0.00065	−1.6	0.00011	RSDTSFMFQRVRISQT-YQQQYGRS	Signal transduction/Ca regulation
1832	P07339	Cathepsin D	6.1	45 037	7/11	18	80/56	−1.44	0.00097	−2.06	8.70×10^{-06}	K.QPGITFIAAK.FR.YYT-VFDRDNNR.V	Protein degradation
1259	P48444	Coatomer subunit δ	5.89	57 630	5/8	10	58/56	−1.72	0.0024	−1.82	0.0012	ENVNLAQIRVLLAAAVCTK	Vascular transport
1804	Q13011	δ(3,5)-δ(2,4)-Dienoyl-CoA isomerase, mitochondrial	8.16	36 136	5/13	19	78/56	−1.44	0.00017	−1.47	1.90×10^{-05}	K.EVDVGLAADVGTLQR.L R.YQETFNVIER.C	Fatty acid biodegradation
2167	P33316	Deoxyuridine 5′-triphosphate nucleotidohydrolase, mitochondrial	9.65	26 975	5/19	27	58/56	1	1	1.33	0.021	RGNVGVVLFNFGKEKHFID-VGAGVIDEDYRG	DNA synthesis/ drug resistance
1813	O43543	DNA-repair protein XRCC2	5.67	32 620	5/17	23	56/56	1.61	0.00013	−1.36	0.0011	K.TEMLYHLTAR.CR.-LVLFATTQTIMQK.A	DNA repair
2283	P30084	Enoyl-CoA hydratase, mitochondrial	8.34	31 823	5/8	18	74/56	−1.31	0.00065	−1.17	0.014	K.HWDHLTQVK.KK.LF-YSTFATDDR.K	Fatty acid biodegradation
1845	O75955	Flotillin-1	7.08	47 554	4/14	14	58/56	−1.46	2.00×10^{-05}	−1.44	0.0015	VSAQYLSEIEMAKEMLAA-ACQMFLGK	Vascular transport
877	P11413	Glucose-6-phosphate 1-dehydrogenase	6.39	59 675	12/24	26	114/56	−1.09	0.014	−1.5	0.00014	RIIVEKPFGRDRLSNHISSLFRE	DNA synthesis/ pentose pathway
288	Q9NXC2	Glucose–fructose oxidoreductase domain-containing protein 1	5.63	43 700	5/12	10	61/56	1.15	0.048	1.56	0.0022	LMSIMGNVLRQAFQDQDDR	Biosynthesis
419	P41250	Glycyl-tRNA synthetase	6.61	83 828	6/15	12	56/56	1.53	0.0026	2.72	0.015	LPFAAAQIGNSFRIMYT-VFEHTFHVR	Protein synthesis
534	P49915	GMP synthase	6.42	77 408	7/21	14	62/56	−1.34	0.0026	−1.56	0.0071	K.DFHKDEVR.IR.VV-YIFGPPVK.E	DNA synthesis
554	Q12931	Heat shock protein 75 kDa, mitochondrial	8.3	80 345	7/18	13	57/57	1.38	0.0021	1.51	0.014	YSNFVSFPLYLNGR-AQLLQPTLEINPR	Protein folding
1981	P04792	Heat shock protein β-1	5.98	22 826	5/16	20	65/56	−1.42	0.016	−1.1	0.39	RQDEHGYISRCRQLSS-GVSEIRH	Protein folding
282	P08238	Heat shock protein HSP 90-β	4.97	83 554	9/20	13	64/56	1.12	0.022	1.52	0.0068	IDIIPNPQERHFSV-EGQLEFR	Protein folding
1563	P22626	Heterogeneous nuclear ribonucleoproteins A2/B1	8.97	37 464	4/8	11	61/56	−1.33	0.0032	−1.86	0.00041	R.NYYEQWGK.LR.-GGNFGFGDSR.G	RNA processing
2184	P37235	Hippocalcin-like protein 1	5.21	22 413	5/20	28	70/56	−1.51	0.021	−1.21	0.098	KFAEHVFRTKLSLEEFIRG	Calcium-dependent regulation
1466	Q3ZCQ8	Mitochondrial import inner membrane translocase subunit TIM50	8.55	39 850	5/12	16	67/56	−1.69	6.40×10^{-06}	−1.36	0.0011	K.TIALNGVEDVR.TK.-QNLFLGSLTSR.L	Protein transport

Table 1 (*continued*)

No.	Accession no.	Protein name	pI	MW	No. match. peptides	Cov. (%)	Score	GEM300/ Ctrol	*t*-Test	GEM1500/ Ctrl	*t*-Test	Matched peptides	Functional classification
1643	P15559	NAD(P)H dehydrogenase 1	8.91	30 905	4/9	25	58/56	1.95	0.0012	1.32	0.041	R.TSFNYAMKEAAAAALK.K	Detoxification/ anti-oxidant defense
1254	P50395	Rab GDP dissociation inhibitor β	6.11	51 087	5/24	12	56/56	−1.54	2.40×10^{-05}	−3.3	7.20×10^{-07}	VTEGSFVYKFLMANGQLVK	Vascular transport
1151	P13489	Ribonuclease inhibitor	4.71	51 766	7/16	26	117/56	−1.86	0.00063	1.01	0.82	R.WAELLPLLQQCQVVR.L R.VNPALAELNLR.S	RNase inhibitor
355	P23921	Ribonucleoside-diphosphate reductase large subunit	6.76	90 925	7/10	11	76/56	19.61	5.90×10^{-08}	35.95	8.60×10^{-08}	KHPDYAILAARIRVLSGE-FQIVNPHLLKD	DNA synthesis
352	P23921	Ribonucleoside-diphosphate reductase large subunit	6.76	90 925	10/16	13	96/56	19.33	0.0014	35.85	0.00071	RLNSAIIYDRDKTGMYYL.T	DNA synthesis
376	P23921	Ribonucleoside-diphosphate reductase large subunit	6.76	90 925	12/22	15	86/56	23.48	0.0023	43.3	0.0012	KVAERPQHMLMRVKLTSM-HFYGWKQ	DNA synthesis
1579	Q8TEQ0	Sorting nexin-29	6.14	48 308	7/10	19	71/56	−1.12	0.13	−1.41	0.00045	R.KDELEEENR.SR.SLRNLLD-GEMEHSAALR.Q	Protein sorting
852	Q9HB58	Sp110 nuclear body protein	9.2	79 765	9/24	18	77/56	−2.05	0.00027	−1.49	0.0015	AMEEALFQHFMHQKVTQGA-ASPGHGIQEK	Gene regulation
662	P29401	Transketolase	7.58	68 519	5/10	12	58/56	1.78	2.50×10^{-05}	−1.04	0.23	RTVPFCSTFAAFFTRART-SRPENAIIYNNNEDFQVGQAKV	Metabolism
665	P29401	Transketolase	7.58	68 519	6/13	15	63/56	1.79	6.90×10^{-05}	−1.02	0.4	KILATPPQEDAPSVDIANIRM KLDNLVAILDINRL	Metabolism
838	O60701	UDP-glucose 6-dehydrogenase	6.73	55 674	7/10	14	78/56	−1.24	0.033	−1.55	0.0083	MLKPAFIFDGRLAANAFLAQR	Biosynthesis
802	O95876	WD repeat-containing protein LOC51057	5.97	86 170	5/7	8	58/56	−1.17	0.41	2.24	0.0039	R.DIGIYQYYDK.KR.-HLAINCVHDR.V	Cytoskeleton regulation
1195	Q96K21	Zinc finger FYVE domain-containing protein 19	5.57	52 411	5/14	13	58/56	1.13	0.088	1.36	0.024	RRDLSSADPAVLGATMESRC REGHDAFELKE	Gene regulation
2000	Q96K21	Zinc finger FYVE domain-containing protein 19	5.57	52 411	5/15	12	60/56	1.55	0.099	1.67	0.052	KWSPPQNYKKRREGHD-AFELKE	Gene regulation

Average ratios of differential expression ($p < 0.05$) across control PANC-1 cells, GEM 300- and GEM1500-resistant PANC-1 lines were calculated from triplicate gels.

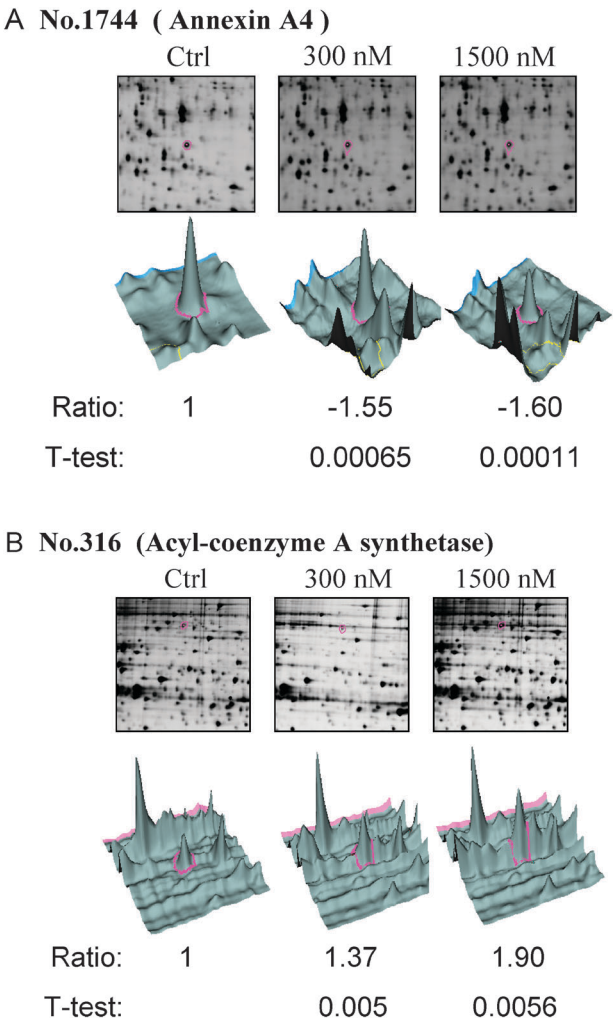

Fig. 2 Representative images of the identified spots (A) annexin A4; (B) acyl-coenzyme A synthetase displaying various levels of gemcitabine resistance-induced protein expression changes. The levels of these proteins were visualized by 2-DE images (top panels), three-dimensional spot images (middle panels), and the ratios of protein expression alterations (bottom panels).

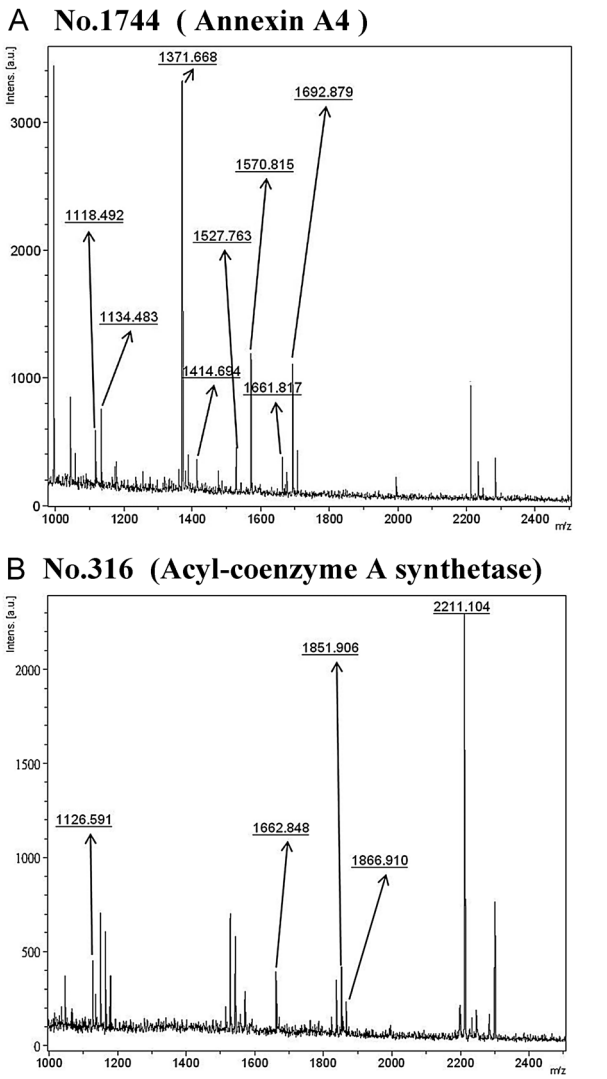

Fig. 3 Peptide mass fingerprint of identified proteins (A) annexin A4; (B) acyl-coenzyme A synthetase. Peptides that contribute to protein identifications are marked with m/z values.

This might provide an explanation for the rapid proliferation of GEM-resistant cells which require more building blocks than GEM-sensitive cells (data not shown). The detoxification protein, NAD(P)H dehydrogenase 1, functions as a cellular antioxidant defense by preventing the formation of reactive oxygen species. NAD(P)H dehydrogenase 1 levels have been shown to upregulate in many tumour types.[24,25] However, no report indicates the relationship between NAD(P)H dehydrogenase 1 and GEM-induced drug resistance in cancer cells. Therefore, we suggest that the downregulation of glucose-6-phosphate 1-dehydrogenase in this study (Table 1), a pentose pathway enzyme, might reduce intracellular reducing power thus increasing the intracellular ROS level. As a result, the NAD(P)H dehydrogenase 1 was upregulated to neutralize excessive ROS. Proteomic analysis combining a triplicate 2D-DIGE system and MALDI-TOF mass spectrometry has been shown here to be useful for confidently detecting intracellular proteins with differential expression in GEM-sensitive- and GEM-resistant-pancreatic epithelial carcinoma. These findings suggest that many of the identified proteins occur within closely related signaling networks and are involved in protein degradation, drug resistance, DNA synthesis, DNA repair, protein folding, RNA processing, and detoxification. Further investigation revealed that many of the identified proteins showed evidence of interplay with the tumor suppressor protein p53 suggesting that the p53 protein might be functionally involved in the mechanism of GEM-induced resistance to chemotherapy.

Proteomic analysis with a large-scale 2D-DIGE system and MALDI-TOF MS identification were shown to be useful for detecting pancreatic proteins with differential expression in pancreatic cancer cell lines that were sensitive or resistant to GEM. Such proteins may be involved in the mechanism of resistance to chemotherapy. Additionally, the identified upregulated proteins could also be possible indicators for predicting the response of pancreatic cancer patients to treatment with GEM and other drugs such as 5-fluorouracil. We have grouped the identified proteins in this study and

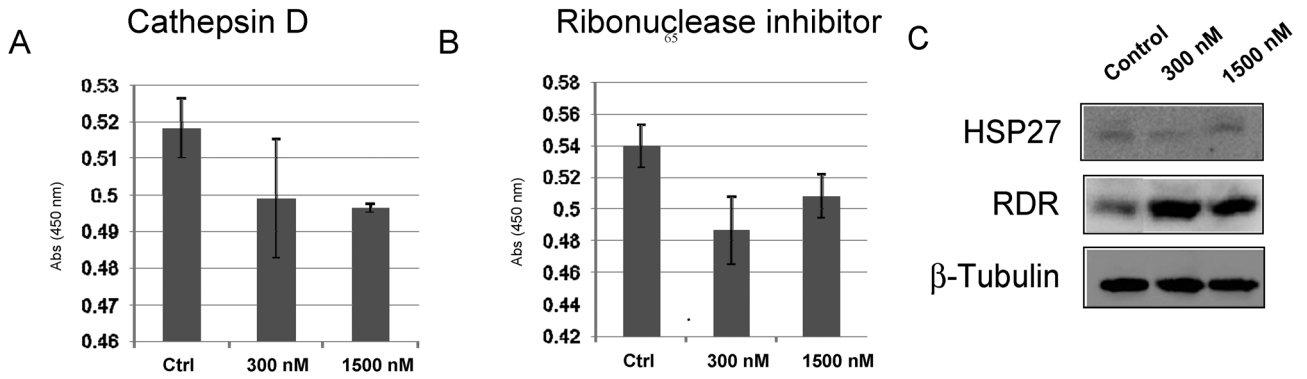

Fig. 4 Representative ELISA and immunoblotting analyses for selected differentially expressed proteins identified by proteomic analysis in various levels of gemcitabine resistant cells. The levels of identified proteins (A) cathepsin D and (B) ribonuclease inhibitor were confirmed by ELISA. The level of the identified protein, (C) heat shock protein β-1 and ribonucleoside-diphosphate reductase, was confirmed by immunoblotting.

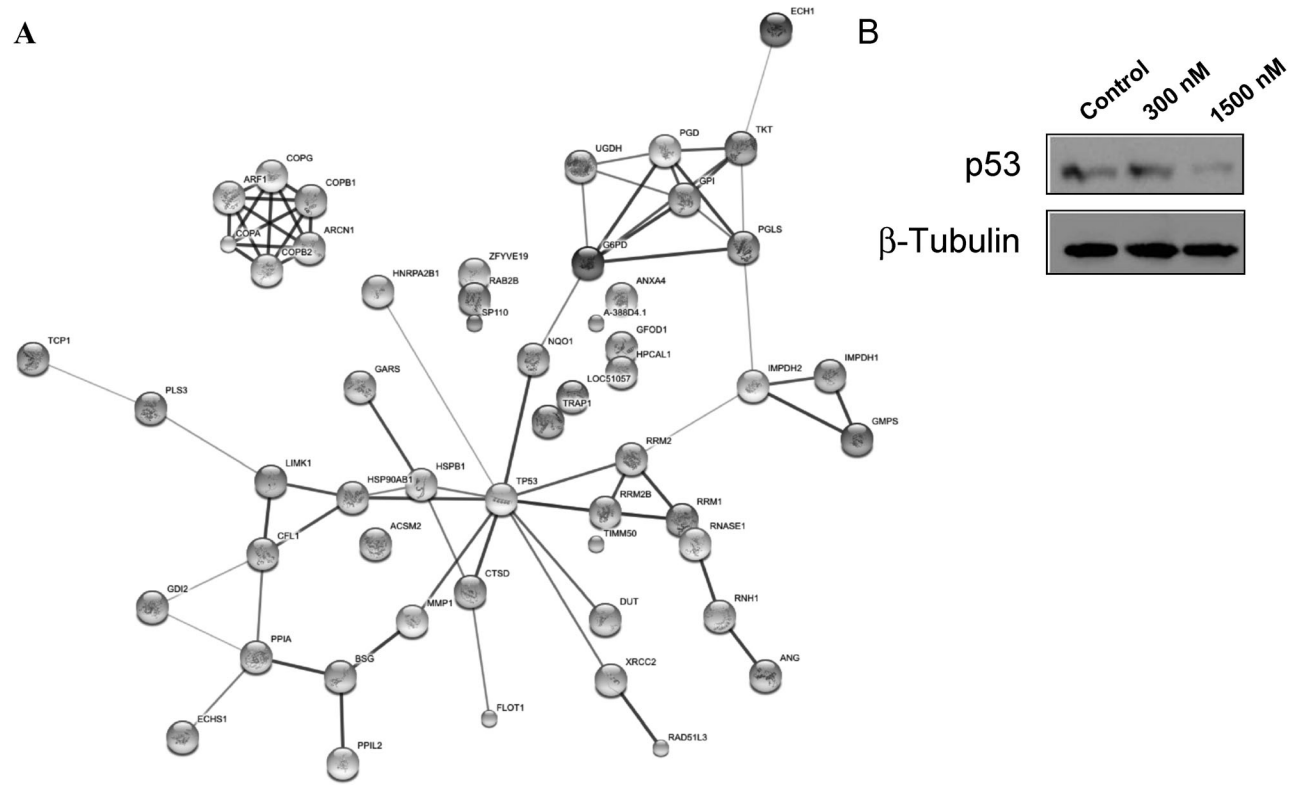

Fig. 5 Interaction networks of identified proteins. (A) The proteins identified in Table 1 were imported into the EMBL Search Tool for the Retrieval of Interacting Proteins (STRING) database (http://string.embl.de/) followed by the addition of 30 closely related partners, and an interaction map was generated. Each node represents a protein entry. Interactions or edges were generated from experimental, text mining and database evidence using the 'medium' confidence level. Thicker lines represent higher confidence interactions. (B) The levels of p53 protein across GEM-sensitive PANC-1 and, GEM 300-, and GEM 1500-resistant PANC-1 lines were determined by immunoblotting analysis.

proposed mechanisms of GEM-induced drug resistance in PANC-1 cells which are summarized in Fig. 6.

Materials and methods

Chemicals and reagents

Generic chemicals were purchased from Sigma-Aldrich (St. Louis, USA), while reagents for 2D-DIGE were purchased from GE Healthcare (Uppsala, Sweden). All primary antibodies were purchased from Abcam (Cambridge, UK) and anti-mouse, and anti-rabbit secondary antibodies were purchased from GE Healthcare (Uppsala, Sweden). All the chemicals and biochemicals used in this study were of analytical grade.

Cell lines and cell cultures

The pancreatic cancer line PANC-1 was purchased from American Type Culture Collection (Manassas, VA) and its

Table 2 List of proteins that potentially contribute to fatty acid synthesis, fatty acid biodegradation, protein synthesis, protein degradation, vascular transport, DNA synthesis, detoxification and calcium-dependent regulation in comparing GEM-resistant PANC-1 cells with GEM-sensitive PANC-1 cells

Functional classification	Trend	Examples
Fatty acid biosynthesis	↑	Acyl-coenzyme A synthetase ACSM2B
Protein synthesis	↑	Glycyl-tRNA synthetase
DNA synthesis	↑	Deoxyuridine 5′-triphosphate nucleotidohydrolase; ribonucleoside-diphosphate reductase
Detoxification	↑	NAD(P)H dehydrogenase 1
Fatty acid biodegradation	↓	δ(3,5)-δ(2,4)-Dienoyl-CoA isomerase; enoyl-CoA hydratase
Protein degradation	↓	Cathepsin D
Vascular transport	↓	Coatomer subunit delta; Flotillin-1; Rab GDP dissociation inhibitor β
Calcium-dependent regulation	↓	Annexin A4; Hippocalcin-like protein 1

Additional details for each protein can be found in Table 1.

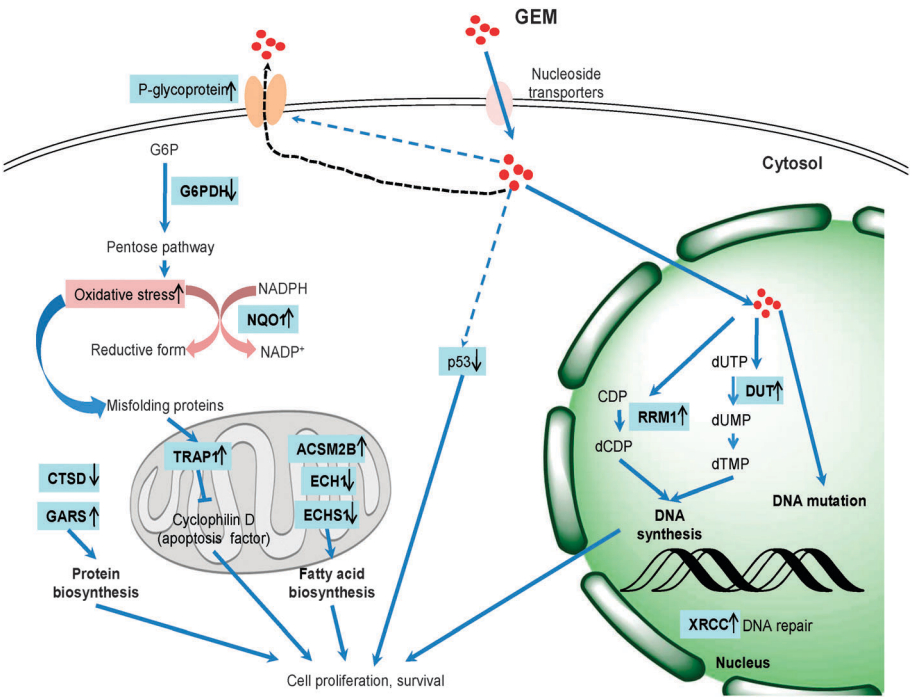

Fig. 6 Model of GEM-induced PANC-1 resistance. The proposed mechanisms suggest that GEM can promote enzymes responsible for DNA synthesis (RRM1 and DUT) and the protein responsible for DNA repair (XRCC). GEM-induced PANC-1 resistant cells may modulate cell proliferation and cell survival *via* stimulating the expression profiling of proteins involved in protein biosynthesis and fatty acid biosynthesis as well as reducing the expression of pro-apoptotic protein, p53, and proteins associated with protein degradation and fatty acid degradation. In addition, GEM-resistant PANC-1 can manage cellular oxidative stress and toxicity by promoting pentose pathway to regenerate NADPH and multiple drug resistant protein, p-glycoprotein. Identified proteins involving this network are highlighted with blue in bold. Identified proteins that were up-regulated and down-regulated in response to GEM-resistance are denoted with "↑" and "↓", respectively.

GEM-resistant lines were established by stepwise increasing the concentration of GEM in culture medium. These resistant PANC-1 cells can be regularly maintained in DMEM medium containing either 300 nM (GEM 300) or 1500 nM (GEM 1500) of GEM, respectively, and supplemented with 10% fetal bovine serum, L-glutamine (2 mM), streptomycin (100 μg mL^{-1}), penicillin (100 IU mL^{-1}) (all from Gibco-Invitrogen Corp., UK). The IC_{50} of GEM-sensitive, GEM 300 and GEM 1500 were 37 nM, 740 nM and 8500 nM, respectively, with a significant increase in the P-glycoprotein level (ESI†).

Sample preparation for proteomic analysis

PANC-1 cells with differential GEM resistances were regularly cultured in medium containing 0 nM, 300 nM and 1500 nM of GEM. These resistant cells were changed to grow in GEM-free medium 2-weeks before the proteomics analysis. Cells at ~80% confluence were washed in chilled 0.5 × PBS and scraped in 2-DE lysis buffer containing 4% w/v CHAPS, 7 M urea, 2 M thiourea, 10 mM Tris-HCl, pH 8.3, 1 mM EDTA. Lysates were homogenized by passage through a 25-gauge needle 10 times, insoluble material was removed by centrifugation at 13 000 rpm for 30 min at 4 °C, and protein concentrations were determined using Coomassie Protein Assay Reagent (BioRad).

2D-DIGE and gel image analysis

Before performing 2D-DIGE, protein samples were labeled with *N*-hydroxy succinimidyl ester-derivatives of the cyanine

dyes Cy2, Cy3 and Cy5 following the protocol described previously.[8,11,12] Briefly, 100 μg of protein sample was minimally labeled with 250 pmol of either Cy3 or Cy5 for comparison on the same 2-DE. To facilitate the image matching and cross-gel statistical comparison, a pool of all samples was also prepared and labeled with Cy2 at a molar ratio of 2.5 pmol Cy2 per μg of protein as an internal standard for all gels. Thus, the triplicate samples and the internal standard could be run and quantified on multiple 2-DE. The labeling reactions were performed for 30 min on ice in the dark and then quenched with a 20-fold molar ratio excess of free L-lysine to dye for 10 min. The differentially Cy3- and Cy5-labeled samples were then mixed with the Cy2-labeled internal standard and reduced with dithiothreitol for 10 min. IPG buffer, pH 3–10 nonlinear (2% (v/v), GE Healthcare), was added and the final volume was adjusted to 450 μl with 2D-lysis buffer for rehydration. The rehydration process was performed with immobilized non-linear pH gradient (IPG) strips (pH 3–10, 24 cm) which were later rehydrated by CyDye-labeled samples in the dark at room temperature overnight (at least 12 hours). Isoelectric focusing was then performed using a Multiphor II apparatus (GE Healthcare) for a total of 62.5 kV h at 20 °C. Strips were equilibrated in 6 M urea, 30% (v/v) glycerol, 1% SDS (w/v), 100 mM Tris-HCl (pH 8.8), 65 mM dithiothreitol for 15 min and then in the same buffer containing 240 mM iodoacetamide for another 15 min. The equilibrated IPG strips were transferred onto 26 × 20 cm 12.5% polyacrylamide gels casted between low fluorescent glass plates. The strips were overlaid with 0.5% (w/v) low melting point agarose in a running buffer containing bromophenol blue. The gels were run in an Ettan Twelve gel tank (GE Healthcare) at 4 Watt per gel at 10 °C until the dye front had completely run off the bottom of the gels. Afterward, the fluorescence 2-DE was scanned directly between the low fluorescent glass plates using an Ettan DIGE Imager (GE Healthcare). This imager is a charge-coupled and device-based instrument that enables scanning at different wavelengths for Cy2-, Cy3-, and Cy5-labeled samples. Gel analysis was performed using DeCyder 2-D Differential Analysis Software v7.0 (GE Healthcare) to co-detect, normalize and quantify the protein features in the images. Features detected from non-protein sources (*e.g.* dust particles and dirty backgrounds) were filtered out. Spots displaying $a \geqq 1.3$ average-fold increases or decreases in abundance with a p-value < 0.05 were selected for protein identification.

Protein staining

Colloidal coomassie blue G-250 staining was used to visualize CyDye-labeled protein features in 2-DE. Bonded gels were fixed in 30% v/v ethanol, 2% v/v phosphoric acid overnight, washed three times (30 min each) with ddH2O and then incubated in 34% v/v methanol, 17% w/v ammonium sulfate, 3% v/v phosphoric acid for 1 h prior to adding 0.5 g L^{-1} coomassie blue G-250. The gels were then left to stain for 5–7 days. No destaining step was required. The stained gels were then imaged on an ImageScanner III densitometer (GE Healthcare), which processed the gel images as .tif files.

In-gel digestion

Excised post-stained gel pieces were washed three times in 50% acetonitrile, dried in a SpeedVac for 20 min, reduced with 10 mM dithiothreitol in 5 mM ammonium bicarbonate pH 8.0 (ammonium bicarbonate) for 45 min at 50 °C and then alkylated with 50 mM iodoacetamide in 5 mM ammonium bicarbonate for 1 h at room temperature in the dark. The gel pieces were then washed three times in 50% acetonitrile and vacuum-dried before reswelling with 50 ng of modified trypsin (Promega) in 5 mM ammonium bicarbonate. The pieces were then overlaid with 10 μl of 5 mM ammonium bicarbonate and trypsinized for 16 h at 37 °C. Supernatants were collected, peptides were further extracted twice with 5% trifluoroacetic acid in 50% acetonitrile and the supernatants were pooled. Peptide extracts were vacuum-dried, resuspended in 5 μl ddH2O, and stored at −20 °C prior to MS analysis.

Protein identification by MALDI-TOF MS

Extracted proteins were cleaved with a proteolytic enzyme to generate peptides, then a peptide mass fingerprinting (PMF) database search following MALDI TOF mass analysis was employed for protein identification. Briefly, 0.5 μl of trypsin digested protein sample was first mixed with 0.5 μl of a matrix solution containing α-cyano-4-hydroxycinnamic acid at a concentration of 1 mg in 1 ml of 50% acetonitrile (v/v)/ 0.1% trifluoroacetic acid (v/v), spotted onto an anchorchip target plate (Bruker Daltonics) and dried. The peptide mass fingerprints were acquired using an Autoflex III mass spectrometer (Bruker Daltonics) in reflector mode. The algorithm used for spectrum annotation was SNAP (Sophisticated Numerical Annotation Procedure). The following detailed metrics were used: peak detection algorithm: SNAP; signal to noise threshold: 25; relative intensity threshold: 0%; minimum intensity threshold: 0; maximal number of peaks: 50; quality factor threshold: 1000; SNAP average composition: averaging; baseline subtraction: median; flatness: 0.8; MedianLevel: 0.5. The spectrometer was also calibrated with a peptide calibration standard (Bruker Daltonics) and internal calibration was performed using trypsin autolysis peaks at m/z 842.51 and m/z 2211.10. Peaks in the mass range of m/z 800–3000 were used to generate a peptide mass fingerprint that was searched against the Swiss-Prot/TrEMBL database (v57.12) with 513 877 entries using Mascot software v2.2.06 (Matrix Science, London, UK). The following parameters were used: homo sapiens; tryptic digest with a maximum of 1 missed cleavage; carbamidomethylation of cysteine, partial protein N-terminal acetylation, partial methionine oxidation and partial modification of glutamine to pyroglutamate and a mass tolerance of 50 ppm. Identification was accepted based on significant MASCOT Mowse scores ($p < 0.05$), spectrum annotation and observed *versus* expected molecular weight and pI on 2-DE.

Immunoblotting

Immunoblotting was used to validate the differential expression of mass spectrometry identified proteins. Cells were lysed with a lysis buffer containing 50 mM HEPES pH 7.4, 150 mM NaCl, 1% NP40, 1 mM EDTA, 2 mM sodium orthovanadate, 100 μg mL^{-1} AEBSF, 17 μg mL^{-1} aprotinin, 1 μg mL^{-1} leupeptin,

1 μg mL^{-1} pepstatin, 5 μM fenvalerate, 5 μM BpVphen and 1 μM okadaic acid prior to protein quantification with Coomassie Protein Assay Reagent (BioRad). 30 μg of protein samples were diluted in Laemmli sample buffer (final concentrations: 50 mM Tris pH 6.8, 10% (v/v) glycerol, 2% SDS (w/v), 0.01% (w/v) bromophenol blue) and separated by 1D-SDS-PAGE following standard procedures. After electroblotting separated proteins onto 0.45 μm Immobilon P membranes (Millipore), the membranes were blocked with 5% w/v skim milk in TBST (50 mM Tris pH 8.0, 150 mM NaCl and 0.1% Tween-20 (v/v)) for 1 h. Membranes were then incubated in primary antibody solution in TBS-T containing 0.02% (w/v) sodium azide for 2 h. Membranes were washed in TBS-T (3 × 10 min) and then probed with the appropriate horseradish peroxidase-coupled secondary antibody (GE Healthcare). After further washing with TBS-T, immunoprobed proteins were visualized using an enhanced chemiluminescence method (Visual Protein Co.).

Enzyme-linked immunosorbent assay (ELISA) analysis of plasma

EIA polystyrene microtitration wells were coated with 50 μg of protein samples and incubated at 37 °C for 2 h. The plate was washed for three times with phosphate buffered saline-Tween 20 (PBST) and three times with PBS. After the uncoated space was blocked with 100 μl of 5% skimmed milk in PBS at 37 °C for 2 h, the plate was washed three times with PBST. Antibody (Abcam) solution was added and incubated at 37 °C for 2 h. After washing with PBST and PBS for 10 times in total, 100 μl of peroxidase-conjugated secondary antibodies in PBS was added for incubation at 37 °C for 2 h. Following 10 washings, 100 μl of 3,3′,5,5′-tetramethylbenzidine (Pierce) was added. After incubation at room temperature for 30 min, 100 μl of 1 M H_2SO_4 was added to stop the reaction followed by measured absorbance at 450 nm using a Stat Fax 2100 microtiterplate reader (Awareness Technology Inc. FL, USA).

Acknowledgements

This work was supported by NSC grant (99-2311-B-007-002 and 100-2311-B-007-005) from National Science Council, Taiwan, NTHU and CGH grant (99N82424E1) from National Tsing Hua University, NTHU Booster grant (99N2908E1) from National Tsing Hua University, Nano- and Micro-ElectroMechanical Systems-based Frontier Research on Cancer Mechanism, Diagnosis, and Treatment grant from National Tsing Hua University and VGHUST grant (99-P5-22) from Veteran General Hospitals University System of Taiwan.

References

1 H. Lage, *Cell Mol. Life Sci.*, 2008, **65**, 3145–3167.
2 R. C. Williamson, *Br. Med. J.*, 1988, **296**, 445–446.
3 D. Li, K. Xie, R. Wolff and J. L. Abbruzzese, *Lancet*, 2004, **363**, 1049–1057.
4 N. M. Cerqueira, P. A. Fernandes and M. J. Ramos, *Chemi.–Eur. J.*, 2007, **13**, 8507–8515.
5 E. Giovannetti, V. Mey, S. Nannizzi, G. Pasqualetti, M. Del Tacca and R. Danesi, *Mol. Cancer. Ther.*, 2006, **5**, 1387–1395.
6 J. F. Timms and R. Cramer, *Proteomics*, 2008, **8**, 4886–4897.
7 H. L. Huang, H. W. Hsing, T. C. Lai, Y. W. Chen, T. R. Lee, H. T. Chan, P. C. Lyu, C. L. Wu, Y. C. Lu, S. T. Lin, C. W. Lin, C. H. Lai, H. T. Chang, H. C. Chou and H. L. Chan, *J. Biomed. Sci. (London, U. K.)*, 2010, **17**, 36.
8 T. C. Lai, H. C. Chou, Y. W. Chen, T. R. Lee, H. T. Chan, H. H. Shen, W. T. Lee, S. T. Lin, Y. C. Lu, C. L. Wu and H. L. Chan, *J. Proteome Res.*, 2010, **9**, 1302–1322.
9 H. C. Chou, Y. W. Chen, T. R. Lee, F. S. Wu, H. T. Chan, P. C. Lyu, J. F. Timms and H. L. Chan, *Free Radicals Biol. Med.*, 2010, **49**, 96–108.
10 H. L. Chan, P. R. Gaffney, M. D. Waterfield, H. Anderle, M. H. Peter, H. P. Schwarz, P. L. Turecek and J. F. Timms, *FEBS Lett.*, 2006, **580**, 3229–3236.
11 H. L. Chan, S. Gharbi, P. R. Gaffney, R. Cramer, M. D. Waterfield and J. F. Timms, *Proteomics*, 2005, **5**, 2908–2926.
12 S. Gharbi, P. Gaffney, A. Yang, M. J. Zvelebil, R. Cramer, M. D. Waterfield and J. F. Timms, *Mol. Cell. Proteomics*, 2002, **1**, 91–98.
13 G. S. Wu, P. Saftig, C. Peters and W. S. El Deiry, *Oncogene*, 1998, **16**, 2177–2183.
14 P. M. Wilson, W. Fazzone, M. J. LaBonte, H. J. Lenz and R. D. Ladner, *Nucleic Acids Res.*, 2009, **37**, 78–95.
15 S. G. Kuznetsov, D. C. Haines, B. K. Martin and S. K. Sharan, *Cancer Res.*, 2009, **69**, 863–872.
16 C. O'Callaghan-Sunol, V. L. Gabai and M. Y. Sherman, *Cancer Res.*, 2007, **67**, 11779–11788.
17 D. Walerych, M. Gutkowska, M. P. Klejman, B. Wawrzynow, Z. Tracz, M. Wiech, M. Zylicz and A. Zylicz, *J. Biol. Chem.*, 2010, **285**, 32020–32028.
18 M. Prahl, A. Vilborg, C. Palmberg, H. Jornvall, C. Asker and K. G. Wiman, *FEBS Lett.*, 2008, **582**, 2173–2177.
19 G. Asher, J. Lotem, L. Sachs, C. Kahana and Y. Shaul, *Proc. Natl. Acad. Sci. U. S. A.*, 2002, **99**, 13125–13130.
20 K. Nakano, E. Balint, M. Ashcroft and K. H. Vousden, *Oncogene*, 2000, **19**, 4283–4289.
21 S. Nakahira, S. Nakamori, M. Tsujie, Y. Takahashi, J. Okami, S. Yoshioka, M. Yamasaki, S. Marubashi, I. Takemasa, A. Miyamoto, Y. Takeda, H. Nagano, K. Dono, K. Umeshita, M. Sakon and M. Monden, *Int. J. Cancer*, 2007, **120**, 1355–1363.
22 L. P. Jordheim, O. Guittet, M. Lepoivre, C. M. Galmarini and C. Dumontet, *Mol. Cancer. Ther.*, 2005, **4**, 1268–1276.
23 J. D. Davidson, L. Ma, M. Flagella, S. Geeganage, L. M. Gelbert and C. A. Slapak, *Cancer Res.*, 2004, **64**, 3761–3766.
24 A. M. Czarnecka, A. Klemba, T. Krawczyk, M. Zdrozny, R. S. Arnold, E. Bartnik and J. A. Petros, *Oncol. Rep.*, 2010, **23**, 531–535.
25 T. Shimada, R. Moriuchi, T. Mori, K. Yamada, T. Ishimaru and S. Katamine, *Biochem. Biophys. Res. Commun.*, 2006, **339**, 852–857.

